Available online at www.sciencedirect.com
SCIENCE DIRECT®

Composites: Part A 37 (2006) 989–996

composites
Part A: applied science and manufacturing

www.elsevier.com/locate/compositesa

A dislocation approach for the thermal stress intensity factors of a crack in an infinite anisotropic medium under uniform heat flow

L. Liu*,[1], G.A. Kardomateas[2]

Georgia Institute of Technology, Atlanta, GA 30332-0150, USA

Abstract

On the basis of the two-dimensional theory of anisotropic thermoelasticity, a solution is given for the thermal stress intensity factors due to the obstruction of a uniform heat flux by an insulated line crack in a generally anisotropic body. The crack is replaced by continuous distributions of sources of temperature discontinuity and dislocations. First, the particular thermoelastic dislocation solutions for an infinite plane are obtained. Then the corresponding isothermal solutions are superposed to satisfy the traction-free conditions on the crack surfaces. The dislocation solutions are applied to calculate the thermal stress intensity factors, which are validated by the exact solutions. The effects of the uniform heat flux, the ply angle and the crack length are investigated.

Keywords: A. Polymer–matrix composites (PMCs); B. Fracture; B. Thermomechanical; C. Analytical modelling

1. Introduction

When a steady heat flow is disturbed by the presence of cracks, large thermal stresses arise in the neighbourhood of the crack tips and may cause crack propagation in structural components. Consequently, the study of the behaviour of the thermal stresses in the vicinity of the crack tips is of great practical importance. Anisotropic media are often encountered in modern technology with the increasing use of composite and sandwich material systems. In particular, thermal stress concentrations around material discontinuities in anisotropic bodies can be induced when composite materials with delaminations are subjected to fire loading.

Solutions of thermal stresses due to a plane crack in an isotropic semi-plane have been published by H. Sekine [1]. He used continuous distributions of sources of temperature discontinuity and edge dislocations to model the insulated line crack along an arbitrary direction. Some basic equations for crack problems in anisotropic thermoelasticity were derived by Clements [2]. Atkinson and Clements [3] gave a solution for the two-dimensional Griffith crack obstructing a uniform heat flux in a general anisotropic medium by the techniques of Fourier transforms and multiple integrations. Sturla and Barber [4,5] considered the same problem in a general anisotropic infinite plane by using a Green's function and gave the exact solutions of the mixed-mode thermal stress intensity factors. They extended their method to the case where the crack is practically close.

From this literature survey, it is obvious that Fourier transforms or the terms of Green's functions to represent the elastic stress and displacement fields have been extensively used in anisotropic thermoelasticity. But this approach requires finding a suitable Fourier transforms or Green's functions associated with the particular distribution of the temperature field or the heat flux and the boundary conditions. For the more complex cases, these approaches may not be suitable and would require a large effort to solve the problem.

In this paper, an alternative dislocation method for an insulated crack in an orthotropic material is presented. Eshelby et al. [6] and Stroh [7] are among the pioneers who presented analytical solutions for a dislocation in general anisotropic materials. Following their work, Atkinson and Eftaxiopoulos [8] achieved the solution for a dislocation in an anisotropic half-plane and a bimaterial infinite plane, using the basic formulation of Stroh [7]. But their work did not deal with thermal effects.

It should be mentioned, in terms of physical sense, that a crack with insulated faces perturbs a heat flux, which is

* Corresponding author.
[1] Graduate Research Assistant.
[2] Professor of Aerospace Engineering.

1359-835X/$ - see front matter
doi:10.1016/j.compositesa.2005.03.013

easily understood. A void or defect in the material can be represented as a dislocation, so a crack can be modelled as a dislocation array and therefore it is reasonable that a dislocation array can perturb a heat flux as a crack does.

Considering the thermal effects, the particular thermoelastic solution for a single dislocation obstructing a uniform heat flux superposed with general isothermal solutions for the infinite medium is given, then the single dislocation solution is applied to an insulated line crack, which is modelled as a distribution of the derived dislocation solution for the infinite medium. The thermal stress intensity factors can be calculated from the dislocation solutions and they are validated by the exact solution of Sturla and Barber [4,5].

2. Formulation

2.1. The temperature field distribution with a single dislocation in an infinite anisotropic plane

Let x_1, x_2, x_3 denote Cartesian coordinates and suppose that a homogenous generally anisotropic material occupies the entire space except for a single dislocation located at an arbitrary position (x_{10}, x_{20}). The configuration is shown in Fig. 1. In a homogenous anisotropic medium, the relation between the heat flux, q_i, and the temperature, T, is given:

$$q_i = -K_{ij}\frac{\partial T}{\partial x_j}, \tag{1}$$

where $i,j = 1, 2, 3$ and the convention of summing over a repeat suffix is used. K_{ij} is the thermal conductivity tensor and it satisfies: $K_{ij} = K_{ji}$. If elastic symmetry with respect to the plane $x_i = 0$, $i = 1, 2, 3$, exists, then $K_{12} = K_{13} = K_{23} = 0$ [2].

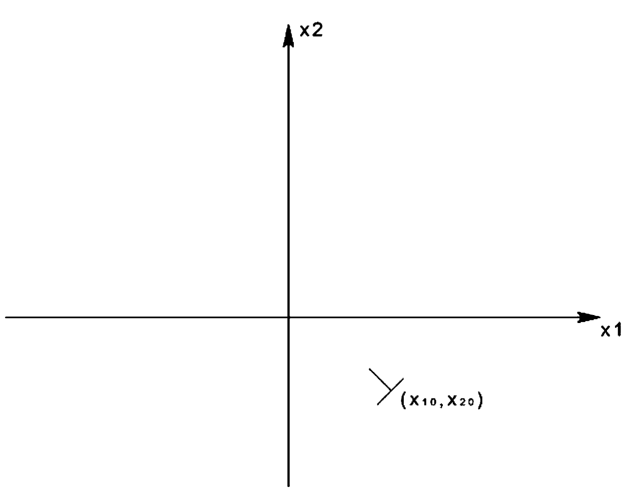

Fig. 1. A dislocation in an anisotropic infinite plane.

The temperature distribution, T, must satisfy the heat conduction equation:

$$-K_{ij}\frac{\partial^2 T}{\partial x_i \partial x_j} = 0, \tag{2}$$

and this can be satisfied by the temperature:

$$T = f(x_1 + \tau x_2) + \bar{f}(x_1 + \bar{\tau} x_2), \tag{3}$$

where τ is the root with positive imaginary part of the equation:

$$K_{11} + 2K_{12}\tau + K_{22}\tau^2 = 0. \tag{4}$$

Then, the temperature may be written as:

$$T = f(z_t) + \bar{f}(\bar{z}_t), \tag{5}$$

where $z_t = x_1 + \tau x_2$ and $f(z_t)$ is an analytic function of z_t.

If ϕ is any function of x_1 and x_2, then the heat flux defined by

$$q_1 = -\frac{\partial \phi}{\partial x_2}; \quad q_2 = \frac{\partial \phi}{\partial x_1}, \tag{6}$$

satisfies Eq. (2) identically. Eqs (1), (5) and (6) then give:

$$\phi = L_t f(z_t) + \bar{L}_t \bar{f}(\bar{z}_t), \tag{7}$$

$$q_1 = -L_t \tau f'(z_t) - \bar{L}_t \bar{\tau} \bar{f}'(\bar{z}_t), \tag{8}$$

$$q_2 = L_t f(z_t) + \bar{L}_t \bar{f}'(\bar{z}_t), \tag{9}$$

where L_t is defined by

$$L_t = -K_{21} - \tau K_{22}. \tag{10}$$

A constant M_t is introduced and defined from the relation

$$M_t L_t = 1. \tag{11}$$

Considering the following temperature distribution:

$$f(z_t) = \frac{1}{4\pi} M_t d_t \log(z_t - \xi_t), \tag{12}$$

which satisfies the singularity of the heat flux at the dislocation point (x_{10}, x_{20}), and where

$$\xi_t = x_{10} + \tau x_{20}, \tag{13}$$

$$t = B_t d_t, \tag{14}$$

$$B_t = \frac{i}{2}(M_t - \bar{M}_t), \tag{15}$$

we can see that along a closed path encircling the dislocation point (x_{10}, x_{20}), the temperature T changes by an amount

$$t = \frac{i}{2}(M_t - \bar{M}_t)d_t = B_t d_t, \tag{16}$$

where t represents the temperature discontinuity strength at the dislocation point (x_{10}, x_{20}). Also, from Eq. (7), the heat flux function corresponding to the temperature

Eq. (12) is:

$$\phi = \frac{1}{4\pi} L_t M_t d_t \log(z_t - \xi_t) + \frac{1}{4\pi} \bar{L}_t \bar{M}_t d_t \log(\bar{z}_t - \bar{\xi}_t). \tag{17}$$

The change in ϕ along a closed path about the point (x_{10}, x_{20}) is:

$$\Delta\phi = \frac{1}{4\pi} L_t M_t d_t (2\pi i) - \frac{1}{4\pi} \bar{L}_t \bar{M}_t \bar{d}_t (2\pi i), \tag{18}$$

which represents the net heat source at the dislocation point. We can see if d_t is real, then $\Delta\phi = 0$. So from Eqs (16) and (18), we can see that the assumed temperature distribution satisfies the constant temperature discontinuity without net heat source at the dislocation point.

2.2. Stress field distribution with a single dislocation for an infinite anisotropic plane

Following Clements [2], we can develop a particular solution for the displacement and temperature fields which would satisfy the equilibrium and heat conduction equations in the form:

$$u_k = C_k g(z_t) + \bar{C}_k \bar{g}(\bar{z}_t), \tag{19}$$

$$T = f(z_t) + \bar{f}(\bar{z}_t), \tag{20}$$

where C_k and $g(z_t)$ can be obtained from:

$$g'(z_t) = f(z_t), \tag{21}$$

$$D_{ik} C_k = \Gamma_i, \tag{22}$$

with D_{ik} and Γ_i given by:

$$D_{ik} = C_{i1k1} + \tau(C_{i1k2} + C_{i2k1}) + \tau^2 C_{i2k2}, \tag{23}$$

$$\Gamma_i = \beta_{i1} + \tau\beta_{i2}. \tag{24}$$

C_{ijkl} and β_{ij} are the elastic constants and the stress-temperature coefficients, respectively. The stress components σ_{ij} can be determined by:

$$\sigma_{ij} = (N_{ij} - \beta_{ij}) f'(z_t) + (\bar{N}_{ij} - \beta_{ij}) \bar{f}'(\bar{z}_t), \tag{25}$$

where

$$N_{ij} = (C_{ijk1} + \tau C_{ijk2}) C_k. \tag{26}$$

The temperature distribution is assumed by Eq. (12), the function is continuous everywhere except at the dislocation point, hence u_k and σ_{ij} are continuous everywhere except at the dislocation point. If we integrate u_k and σ_{ij} along a closed path encircling the dislocation point, the change of the displacement and stress cannot equal to zero. These discontinuities are unacceptable for the particular thermoelastic solutions. Therefore a corrective isothermal solution for the single dislocation should be superposed on the particular solution to restore continuity of stress and displacement at the dislocation point. Following Sturla and Barber [4,5], considering the corrective isothermal solution superposed on the particular thermoelastic solution, the stress σ_{i2} due to the heat flux is given by:

$$\sigma_{i2}^{p} = Q_i f(z_t) + \bar{Q}_i \bar{f}(\bar{z}_t), \tag{27}$$

where

$$Q_i = \sum_{\alpha} \frac{L_{i\alpha} A_{k\alpha}}{L_{j\alpha} A_{j\alpha}} \left(\frac{N_{k2} + \bar{N}_{k2}}{2} - \beta_{k2} \right) + \sum_{\alpha} \frac{L_{i\alpha} L_{k\alpha}}{L_{j\alpha} A_{j\alpha}} \left(\frac{C_k + \bar{C}_k}{2} \right) + N_{i2}. \tag{28}$$

and $A_{k\alpha}$ and $L_{i\alpha}$ are given by Stroh [7].

2.3. Dislocation solutions for an insulated crack in an infinite anisotropic plane

Considering a fully open crack of length $2a$ under uniform heat flux in an infinite anisotropic plane, the configuration is shown in Fig. 2. The crack remains fully open and hence is free of tractions, and also prevents the transfer of heat between its faces. The configuration can be

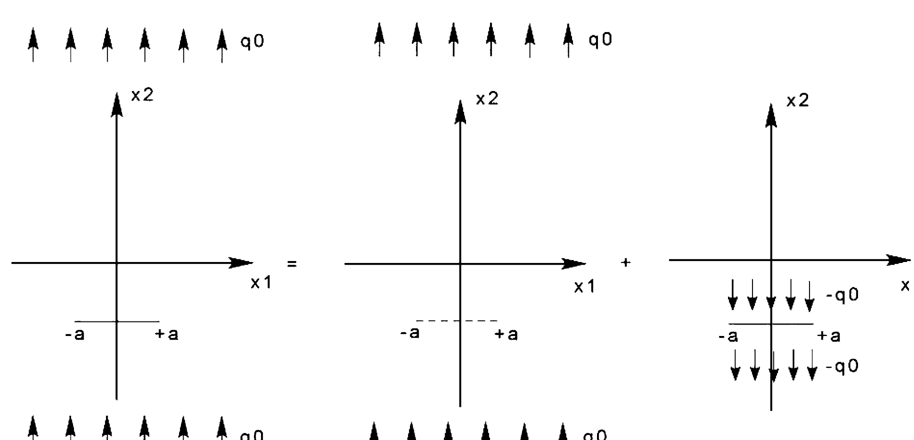

Fig. 2. The thermoelastic plane crack.

decomposed into two configurations; the first one is the one with no crack, which involves no thermal stress; for the second one, the boundary conditions can be written as:

$$q_2 = q_0; \quad -a < x_1 < a, \quad x_2 = x_{20}, \tag{29}$$

$$\sigma_{i2} = 0; \quad -\alpha < x_1 < a, \quad x_2 = x_{20}, \tag{30}$$

$$q_2 = 0; \quad \sqrt{x_1^2 + x_2^2} \to \infty, \tag{31}$$

$$\sigma_{i2} = 0; \quad \sqrt{x_1^2 + x_2^2} \to \infty. \tag{32}$$

For the second configuration, the tractions along the crack surface due to the heat flux $-q_0$ should be calculated first and it is associated by the temperature field distribution.

The temperature field T and heat flux field q_i distribution with a single dislocation for an infinite plane can be determined by Eqs (8), (9) and (12). The crack can be modelled as a series of dislocations with the temperature discontinuity strength $t(s, x_{20})$. Then the heat flux q_2 due to the dislocation series is:

$$q_2^d(x_1, x_{20}) = \int_{-a}^{+a} \tilde{q}_2(x_1, x_{20}, s, x_{20}) t(s, x_{20}) \mathrm{d}s = -q_0(x_1, x_{20}), \tag{33}$$

where $\tilde{q}_2(x_1, x_{20}, s, x_{20})$ is the heat flux at the position (x_1, x_{20}) due to the unit temperature discontinuity strength at the dislocation point (s, x_{20}), so $\tilde{q}_2(x_1, x_{20}, s, x_{20})$ can be calculated from Eq. (9) by setting the unit temperature discontinuity strength at the dislocation point. Eq. (33) should equal to the opposite of the external heat flux to satisfy the free heat flux along the crack surfaces. Since both ends of the crack are singular, we use the case I Gaussian formula [9] to solve Eq. (33), which can be transformed to $N-1$ linear algebraic equations:

$$\pi a \tilde{q}_2(x_{1,k}, x_{20}, s_m, x_{20}) W_m \tilde{t}(\tilde{s}_m, x_{20}) = -q_0(x_{1,k}, x_{20}); \; k = 1, 2 \ldots N-1; \; m = 1, 2 \ldots N \tag{34}$$

where s_m are the integration points, $x_{1,k}$ are the collocation points, W_i are the weight functions appropriate to the quadrature formula employed and N is the number of integration points. These are given by:

$$s_m = a\tilde{s}_m; \quad x_{1,k} = a\tilde{t}_k; \quad \tilde{t}(\tilde{s}_m, x_{20}) = \frac{t(\tilde{s}_m, x_{20})}{\sqrt{1 - \tilde{s}_m^2}}, \tag{35}$$

$$\tilde{s}_m = \cos\left[\frac{\pi(2m-1)}{2N}\right]; \quad \tilde{t}_k = \cos\left[\pi\left(\frac{k}{N}\right)\right]; \quad W_m = \frac{1}{N}. \tag{36}$$

The temperature continuity outside the crack (i.e. $x_1 > a$) can be imposed by enforcing the auxiliary condition:

$$\int_{-a}^{+a} t(s) \mathrm{d}s = 0, \tag{37}$$

which can impose three additional linear equations:

$$\sum_{m=1}^{N} W_m \tilde{t}(\tilde{s}_m, x_{20}) = 0. \tag{38}$$

Eqs. (34) and (38) enable us to calculate the temperature discontinuity strength at the N integration points.

The tractions along the crack surfaces due to the heat flux can be determined from:

$$\sigma_{ij}^t(x_1, x_{20}) = \int_{-a}^{+a} \sigma_{ij}^p(x_1, x_{20}, s, x_{20}) \mathrm{d}s, \tag{39}$$

where the equation has a *Generalized* Cauchy kernel, i.e. $\sigma_{ij}^p(x_1, x_{20}, s, x_{20})$ represents the particular solution for stress distribution due to the heat flux along the crack surfaces; it becomes unbounded as both the integration and collocation variables, s and x_1, tend to the same end-point. Since the temperature discontinuity strength function $t(s, x_{20})$ is singular at each end-point, we can reduce Eq. (39) to a system of algebraic equations [9]:

$$\sigma_{ij}^t(x_{1,k}, x_{20}) = \sum_{m=1}^{N} \sigma_{ij}^p(x_{1,k}, x_{20}, s_m, x_{20}), \tag{40}$$

where $\sigma_{ij}^p(x_{1,k}, x_{20}, s_m, x_{20})$ represents the stress at collocation point $(x_{1,k}, x_{20})$ due to the temperature discontinuity strength at integration point (s_m, x_{20}). So Eq. (40) can be evaluated from Eq. (27) by substituting the temperature discontinuity strength at the N integration points.

To satisfy the traction-free boundary condition at the crack surfaces, we superpose a solution of the corresponding isothermal problem with tractions equal and opposite to those of Eq. (40). This solution is conveniently represented by a distribution of dislocations of strength $b_i(s)$. The solution with a single dislocation $b_i(s)$ for an infinite anisotropic plane is given by Stroh [7], the corresponding stress and displacement distribution is:

$$u_k = \sum_\alpha A_{k\alpha} f_\alpha(z_\alpha) + \sum_\alpha \bar{A}_{k\alpha} \bar{f}_\alpha(\bar{z}_\alpha), \tag{41}$$

$$\sigma_{i1} = -\sum_\alpha L_{i\alpha} p_\alpha f'_\alpha(z_\alpha) - \sum_\alpha \bar{L}_{i\alpha} \bar{p}_\alpha \bar{f}'_\alpha(\bar{z}_\alpha), \tag{42}$$

$$\sigma_{i2} = \sum_\alpha L_{i\alpha} f'_\alpha(z_\alpha) + \sum_\alpha \bar{L}_{i\alpha} \bar{f}'_\alpha(\bar{z}_\alpha). \tag{43}$$

For the infinite medium, we can assume:

$$f(z_\alpha) = \frac{1}{4\pi} M_{\alpha j} d_j \log(z_\alpha - \xi_\alpha), \tag{44}$$

where

$$z_\alpha = x_1 + p_\alpha x_2, \tag{45}$$

$$b_i = B_{ij} d_j, \tag{46}$$

$$B_{ij} = \frac{i}{2}(A_{i\alpha} M_\alpha j - \bar{A}_{i\alpha} \bar{M}_{\alpha j}). \tag{47}$$

Cracks can be modelled as a series of dislocation with the densities $b_i(s, x_{20})$ as well. The tractions along the crack surfaces due to the dislocation series are given:

$$\sigma^d_{ij}(x_1,x_{20}) = \int_{-a}^{+a} \tilde{F}_{ij}(x_1,x_{20},s,x_{20})b_i(s,x_{20})\mathrm{d}s,\ ij = 21,22,23 \tag{48}$$

which equal to the tractions along the crack surfaces due to the heat flux to satisfy the traction-free condition. $\tilde{\mathbf{F}}(x_1,x_{20},s,x_{20})$ represents the stress at the point (x_1, x_{20}) due to the unit dislocation density $\mathbf{b}(\mathbf{s},\ \mathbf{x_{20}})$, it can be obtained by Eqs (42) and (43) by setting $\mathbf{b}=\{1,0,0\}$, $\mathbf{b}=\{0,1,0\}$ and $\mathbf{b}=\{0,0,1\}$, respectively; we use the case I Gaussian formula [9] to solve Eq. (48), which can be transformed to $3(N-1)$ linear algebraic equations:

$$\pi a\tilde{F}_{ij}(x_{1,k},x_{20},s_m,x_{20})\langle\langle W_m,W_m,W_m\rangle\rangle\tilde{b}_i(\tilde{s}_m,x_{20}) = -\sigma^t_{ij}(x_{1,k},x_{20}), \tag{49}$$

where $x_{1,k}$, s_m, W_m are given by Eq. (35) and

$$\tilde{\mathbf{b}}(\tilde{s}_m,x_{20}) = \frac{\mathbf{b}(\tilde{s}_m,x_{20})}{\sqrt{1-\tilde{s}_m^2}}. \tag{50}$$

In addition, it is necessary to impose the closure condition, which gives three additional equations:

$$\sum_{m=1}^{N} W_m\tilde{b}_l(\tilde{s}_m,x_{20}) = 0;\ l = 1,2,3 \tag{51}$$

Eqs. (49) and (51) enable us to calculate the dislocation densities $\tilde{\mathbf{b}}(\tilde{s}_m,x_{20})$ at the N integration points. Then the crack tip dislocation densities can be extrapolated from the N integration points as:

$$\bar{b}_l(1,y_t) = M_E\sum_{m=1}^{N} b_E^{(+1)}\bar{b}_l(\bar{s}_m,y_t), \tag{52}$$

$$\bar{b}_l(-1,y_t) = M_E\sum_{m=1}^{N} b_E^{(-1)}\bar{b}_l(\bar{s}_{N+1-m},y_t), \tag{53}$$

where

$$b_E^{(+1)} = \sin\left[\frac{2m-1}{4N}\pi(2N-1)\right]\Big/\sin\left(\frac{2m-1}{4N}\pi\right);\quad b_E^{(-1)} = b_E^{(+1)};\quad M_E = \frac{1}{N}. \tag{54}$$

$l=1,2,3$ [9].

The stress intensity factors at the crack tip can be calculated as (Huang and Kardomateas, [10]):

$$K_i(+1) = \frac{\sqrt{\pi a}}{2}\ \mathrm{Re}\{L_{i\alpha}M_{\alpha j}B^{-1}_{j\gamma}\tilde{b}_\gamma(+1)\}, \tag{55}$$

$$K_i(-1) = -\frac{\sqrt{\pi a}}{2}\ \mathrm{Re}\{L_{i\alpha}M_{\alpha j}B^{-1}_{j\gamma}\tilde{b}_\gamma(-1)\}, \tag{56}$$

where Re[ ] stands for the real part of a complex variable and $\tilde{b}_\gamma(\pm1)$ are solved from Eqs. (52) and (53).

3. Results and discussion

First, to validate this method presented above, we compared the results with the exact solutions given by Sturla and Barber [4,5]. They gave the thermal stress intensity factors for full-open crack in a general anisotropic infinite plane under uniform heat flux. The solutions are given as:

$$K_I = \lim_{x_1\to a}\sqrt{2\pi(x_1-a)}\sigma_{22} = \frac{q_0G_2}{K}\left(\frac{a}{2}\right)^{3/2}, \tag{57}$$

$$K_{II} = \lim_{x_1\to a}\sqrt{2\pi(x_1-a)}\sigma_{12} = \frac{q_0G_1}{K}\left(\frac{a}{2}\right)^{3/2}, \tag{58}$$

$$K_{III} = \lim_{x_1\to a}\sqrt{2\pi(x_1-a)}\sigma_{32} = \frac{q_0G_3}{K}\left(\frac{a}{2}\right)^{3/2}, \tag{59}$$

where G_i and K are material constants.

The elastic material properties for graphite/epoxy are listed in Table 1. The fiber orientation θ of the lamina is defined as the angle between the x_1 direction and the lamina's longitudinal direction; also x_2 is the normal direction of the thickness of the lamina and the x_3 direction is determined by the right-hand rule.

The convergence of the numerical integration method is very important, this is our first check and convergence studies were done for a 0, 45 and 90° materials. Illustrative results are listed in Table 2 for the 45° homogeneous anisotropic laminate. Notice that the mode I stress intensity factors are zero for all three materials and the mode III stress intensity factors are zero for the 0 and 90° materials. We assume the length of the crack $a=1$ mm and the uniform heat flux $q_0=1.0$ W/m^2. From this table, we can see that the present results agree very well with the analytical solutions.

As the number of integration points increases, the numerical results converge with the analytical results quickly. When $N>100$, the numerical result is acceptable compared with the analytical solution. For illustration, in Fig. 3 the convergence of the method with the number of the integration points is shown as well. We can obtain excellent agreements with the analytical results when the number of integration points $N>100$.

Table 1
Material properties for graphite/epoxy laminate

$E_{11}=144.23$ GPa, $E_{22}=9.65$ GPa, $E_{33}=9.65$ GPa
$G_{12}=4.14$ GPa, $G_{13}=4.14$ GPa, $G_{23}=3.45$ GPa
$\nu_{12}=0.301$, $\nu_{13}=0.301$, $\nu_{23}=0.49$
$\alpha_{11}=0.88$ μm/m K, $\alpha_{22}=31.0$ μm/m K, $\alpha_{33}=31.0$ μm/m K
$K_{11}=4.48$ W/m K, $K_{22}=3.21$ W/m K, $K_{33}=3.21$ W/m K

11 is the longitudinal direction (fiber direction), 33 the transverse, and 22 the normal direction.

Table 2
Convergence of K_{II} and K_{III} for a fully open crack ($m^{1/2}$ Pa)

N	K_{II}			K_{III}		
	Present	Analytical	Error %	Present	Analytical	Error %
10	0.39651	0.42615	6.95397	0.11191	0.12027	6.95429
50	0.42024	0.42615	1.38638	0.11860	0.12027	1.38687
100	0.42319	0.42615	0.69319	0.11944	0.12027	0.69343
150	0.42418	0.42615	0.46205	0.11972	0.12027	0.46229
200	0.42467	0.42615	0.3466	0.11985	0.12027	0.34672
250	0.42496	0.42615	0.27714	0.11994	0.12027	0.27771
300	0.42516	0.42615	0.23114	0.11999	0.12027	0.23114
350	0.4253	0.42615	0.19805	0.12003	0.12027	0.19789
400	0.42541	0.42615	0.17318	0.12006	0.12027	0.17377
450	0.42549	0.42615	0.15394	0.12009	0.12027	0.15465
500	0.42555	0.42615	0.13869	0.12010	0.12027	0.13885
550	0.42561	0.42615	0.12601	0.12012	0.12027	0.12638
600	0.42565	0.42615	0.11545	0.12013	0.12027	0.11557
650	0.42569	0.42615	0.10654	0.12014	0.12027	0.10726
700	0.42572	0.42615	0.09903	0.12015	0.12027	0.09894
750	0.42575	0.42615	0.09246	0.12016	0.12027	0.09229
800	0.42578	0.42615	0.08659	0.12017	0.12027	0.08647

N is the number of integration points.

Fig. 4 displays the influence of the uniform heat flux. The number of integration points $N=300$ and the length of the crack is $a=1$ mm. A 0° homogeneous anisotropic laminate is used in the analysis. From this figure, it can be seen that the thermal stress intensity factors increase with the heat flux linearly. The conclusion agrees with the analytical solutions.

Fig. 5 gives the mode II stress intensity factors for full-open cracks with the crack length from 0.5 to 5 mm. We assume the uniform heat flux is $q_0=1.0\ \mathrm{W/m^2}$ and the number of integration points $N=300$. It can be seen that material anisotropy affects the mode II stress intensity factors. The 0° material gives the highest K_{II}, and the 90° material gives the lowest K_{II}.

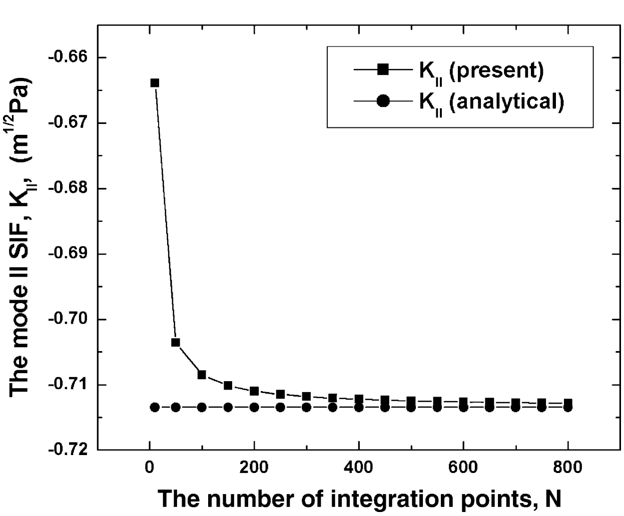

Fig. 3. The convergence of the mode II SIF (0°).

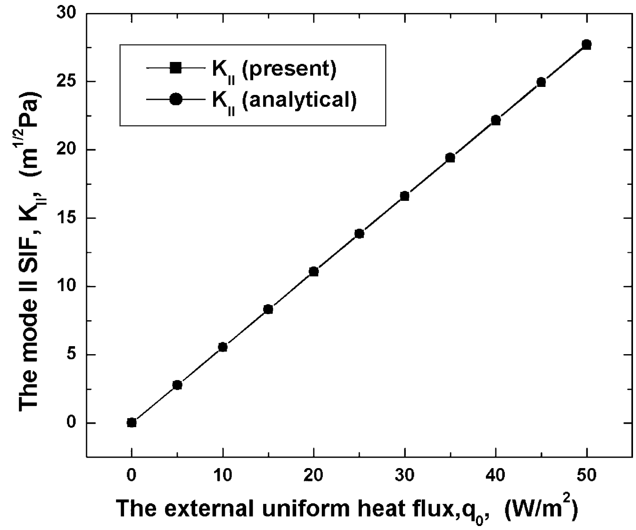

Fig. 4. The Mode-II SIF for a 0° laminate as a function of the uniform external heat flux q_0.

As for the mode mixities ψ, which are defined as:

$$\psi_{II} = \tan^{-1}\left(\frac{K_{II}}{K_I}\right), \quad \psi_{III} = \tan^{-1}\left(\frac{K_{III}}{K_I}\right) \tag{60}$$

The mode I stress intensity factors are zero for all three anisotropic materials under the uniform external heat flux q_0 without the external tensile load. In order to check the mode mixities, the external unit uniform tensile load and heat flux load are applied together. It was proved that the uniform tensile load cannot affect the K_{II} and K_{III} stress intensity factors. Fig. 6 displays the mode-II mode mixities for fully open cracks with the crack length from 0.5 to 5 mm as well. It can be seen that the material anisotropy affects the mode mixities as well. The mode mixities increase quickly as

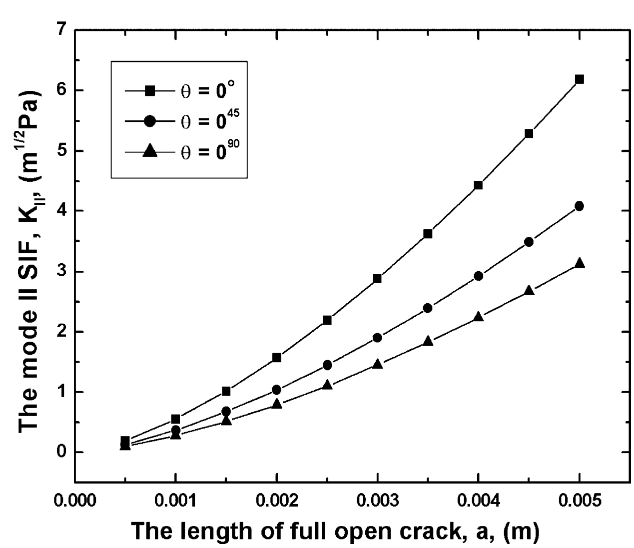

Fig. 5. The Mode-II SIF for a fully open crack in an infinite plane as a function of the crack length.

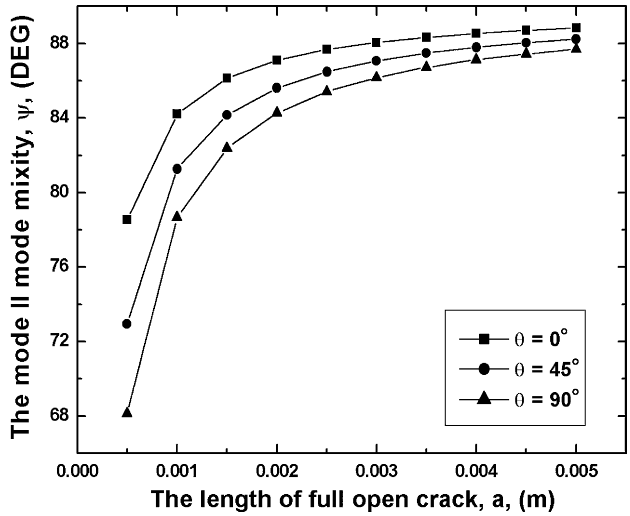

Fig. 6. The Mode-II mode mixity for a fully open crack in an infinite plane as a function of the crack length.

the length of cracks increases for all three anisotropic materials, which indicates that the crack is prone to propagate away from the original crack orientation and the mode-II crack propagation is in dominance.

The effect of fiber angle on the stress intensity factors of the cracks is also studied and the results are shown in Fig. 7. We assume the uniform heat flux is $q_0 = 1.0\ \mathrm{W}/m^2$ and the number of integration points $N = 300$ again. As shown in Fig. 7, the effect of fiber orientation on the mode-II stress intensity factors is seen to be significant at 10 and 20° and depends also on the length of the crack. For other fiber orientations, the effect on the mode II stress intensity factor is rather small.

It should be mentioned that in this paper the solid is treated as a fully anisotropic body, albeit homogeneous. Therefore, an important characteristic of composite construction, namely anisotropy, is taken into account. Our study does not look at individual fibers, i.e. the composite is 'homogeneized', which is a routine assumption made in composite fracture analyses. Using this approach has been indeed found effective in many composite configurations and able to predict the experimentally observed growth of delaminations in both monotonic and cyclic (fatigue)loading (Kardomateas et al. [11]).

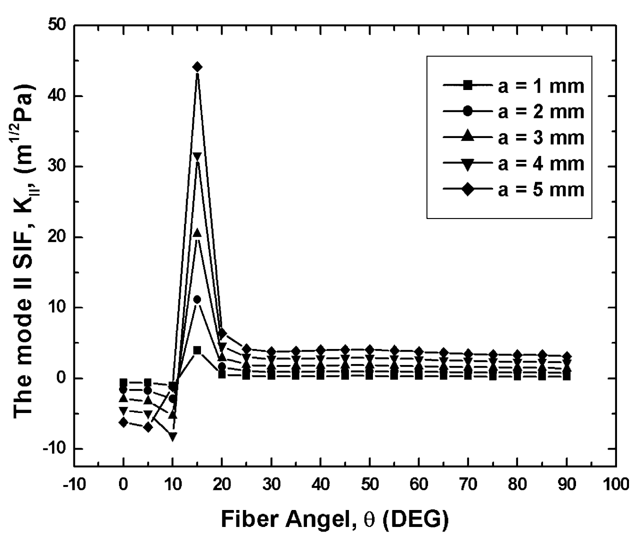

Fig. 7. The effect of fiber angle on the mode II SIF of a fully open crack in an infinite plane.

Finally, the paper deals with anisotropy as far as the elastic deformation, but anisotropy of crack growth resistance is very important as well. This issue will be studied in the future by performing experiments to obtain specific material parameters, which can be used to define crack growth resistance for anisotropic materials.

4. Conclusions

Solutions for the thermal stress intensity factors of fully open cracks in a homogenous general anisotropic infinite plane subjected to a uniform heat flux are derived based on the analytical dislocation approach. The crack is modelled as a series of sources of temperature discontinuity and dislocations. The accuracy and convergence are verified by comparing with the analytical method. The convergence of the numerical method is very satisfactory. Results are presented on the effects of the uniform heat flux, the ply angle and the crack length.

The great advantage of this method is that it can be used for complicated models such as the half-plane, the bimaterial infinite plane, the strip and so on. It can also be used to solve the problem with complicated external loads, including heat and mechanical loads. It is more general and more widely applicable compared with the analytical method because the basic formula is derived from a single dislocation model, which is relatively easy to obtain and satisfy boundary conditions.

Acknowledgements

The financial support of the Office of Naval Research, Grant N00014-03-1-0189, and the interest and encouragement of the Grant Monitors, Dr Patrick C. Potter and Dr Luise Couchman are gratefully acknowledged.

References

[1] Sekine H. Thermal stresses near tips of an insulated line crack in a semi-infinite medium under uniform heat flow. Eng Fract Mech 1977; 9:499–507.

[2] Clements DL. Thermal stress in an anisotropic elastic half-space. SIAM J Appl Math 1973;23(3):332–7.
[3] Atkinson C, Clements DL. On some crack problems in anisotropic thermoelasticity. Int J Solids Struct 1977;12:855–64.
[4] Sturla FA, Barber JR. Thermoelastic Green's functions for plane problems in general anisotropy. ASME J Appl Mech 1988;55:245–7.
[5] Sturla FA, Barber JR. Thermal stresses due to a plane crack in general anisotropic material. ASME J Appl Mech 1988;55:372–6.
[6] Eshelby JD, Read WT, Shockley W. Anisotropic elasticity with application to dislocation theory. Acta Metall 1953;2:251–9.
[7] Stroh AN. Dislocations and cracks in anisotropic elasticity. Philos Mag 1958;3:P625–P46.
[8] Atkinson C, Eftaxiopoulos DA. Interaction between a crack and a free or welded boundary in media with arbitrary anisotropy. Int J Fract 1991;50:159–82.
[9] Hills DA, Kelly PA, Di DN, Korsunsky AM. Solution of crack problems; the distributed dislocation technique. UK: Kluwer Academic Publishers; 1996.
[10] Huang H, Kardomateas GA. Mixed-mode stress intensity factors for cracks located at or parallel the interface in bi-material half planes. Int J Solids Struct 2001;38:3719–34.
[11] Kardomateas GA, Pelegri AA, Malik B. Growth of internal delaminations under-cyclic compression in composite plates. J Mech Phys Solids 1995;43(6):847–68.